Accepted Manuscript

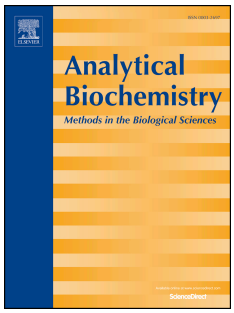

Spectrophotometric method for simultaneous measurement of zinc and copper in metalloproteins using 4-(2-pyridylazo)resorcinol

Colleen Doyle, Dalia Naser, Heather Bauman, Jessica Rumfeldt, Elizabeth Meiering

PII: S0003-2697(18)31267-3

DOI: https://doi.org/10.1016/j.ab.2019.03.007

Reference: YABIO 13273

To appear in: *Analytical Biochemistry*

Received Date: 19 December 2018

Revised Date: 4 March 2019

Accepted Date: 17 March 2019

Please cite this article as: C. Doyle, D. Naser, H. Bauman, J. Rumfeldt, E. Meiering, Spectrophotometric method for simultaneous measurement of zinc and copper in metalloproteins using 4-(2-pyridylazo)resorcinol, *Analytical Biochemistry* (2019), doi: https://doi.org/10.1016/j.ab.2019.03.007.

Spectrophotometric method for simultaneous measurement of zinc and copper in metalloproteins using 4-(2-pyridylazo)resorcinol

*Colleen Doyle[a], Dalia Naser[a] ,Heather Bauman[a,1], Jessica Rumfeldt[a,2], Elizabeth Meiering[a]**

[a]Department of Chemistry, University of Waterloo, Waterloo, Canada.

[1]Present address: Department of Informatics and Life Sciences, Conestoga College, Kitchener, Canada.

[2] Present address: Department of Biological and Environmental Science, University of Jyväskylä, Jyväskylä, Finland.

***Corresponding Author**

E-mail: meiering@uwaterloo.ca

Phone: (519) 888-4567 Ext. 32254

Address: Department of Chemistry
University of Waterloo
200 University Ave W.
Waterloo, ON
N2L 3G1

FUNDING SOURCES

This work was supported by the Canadian Institutes of Health Research (CIHR) and National Sciences and Engineering Research Council of Canada (NSERC).

NOTES

The authors declare no competing financial interests.

SUBJECT CATEGORY

Physical techniques

ABSTRACT

Bound metals are observed in a great many natural proteins, where they perform diverse roles in determining protein folding, stability and function. Due to the diverse impact of bound metals on biophysical and biochemical properties of proteins, it is valuable to have accurate and facile methods for determining the metal content of proteins. Here we describe an optimized methodology using 4-(2-pyridylazo)resorcinol (PAR) to simultaneously quantify two metal ions in solution. The assay is demonstrated for quantification of Cu^{2+} and Zn^{2+} ions in human Cu, Zn superoxide dismutases (SOD1s); however, the method is general and can be applied to various combinations of metal ions. Advantages of the assay are that it is rapid and inexpensive, requires little sample and preparation, and has simple data analysis. We show that spectral decomposition software can accurately resolve the absorption bands of Cu^{2+} and Zn^{2+} with high accuracy and precision. Using the PAR assay, we determined that metal binding is altered in disease-associated mutants of SOD1, with comparable results to those determined by ICP-AES. In addition, we highlight key issues for using spectrophotometric chelators such as PAR for metal analysis of proteins.

KEYWORDS *(max 6 keywords)*

metalloprotein, 4-(2-pyridylazo)resorcinol, PAR, SOD1, metal quantitation, assay

LIST OF ABBREVIATIONS

A_{500}, absorbance at 500 nm; AAS, atomic absorption spectroscopy; ALS, amyotrophic lateral sclerosis; DSC, differential scanning calorimetry; EDTA, ethylenediaminetetraacetic acid; GdnHCl, guanidine hydrochloride; ICP-AES, inductively coupled plasma atomic emission spectroscopy; ICP-MS, inductively coupled plasma mass spectrometry; K_d, dissociation constant; NTA, nitrilotriacetic; PAR, 4-(2-pyridylazo)resorcinol; PAR:Cu^{2+}, PAR with bound Cu^{2+}; PAR_2:Zn^{2+}, PAR with bound Zn^{2+}; pWT, pseudo wild-type SOD1 double mutant used as the control protein; SOD1, human Cu, Zn superoxide dismutase; SpLab, spectral decomposition software; T_m, temperature where half of the protein is unfolded; Zincon, 2-carboxy-2'-hydroxy-5'-sulfoformazylbenzene; λ_{max}, wavelength of maximum absorption

1. Introduction

Bound metals are found in approximately one third of all natural proteins [1], in diverse structural contexts and functional roles [2]. Measurement of the metal content of proteins is complicated by various factors including the complex structure of proteins, which may interfere with quantification, and the generally limited quantities of metal ions in protein samples. For these reasons, selective and sensitive methods are required. Well-known detection methods for metal determination in proteins include atomic absorption spectroscopy (AAS), inductively coupled plasma atomic emission spectroscopy (ICP-AES) and inductively coupled plasma mass spectrometry (ICP-MS). In general, these methods are accurate and reliable but they are typically time-consuming, costly, and are not always easily accessible [3–5].

Alternative methods for quantitating metal ions in metalloproteins make use of chromophores exhibiting altered spectral properties upon metal binding, such as 2-carboxy-2'-hydroxy-5'-sulfoformazylbenzene (Zincon) and 4-(2-pyridylazo)resorcinol (PAR) [6–10]. These chromogenic chelators are inexpensive, fast and easy to use, and sensitive but are often not very selective [11,12] . Due to the low selectivity, their use in metal determination has commonly been restricted to samples containing just one metal ion [13–15]. Still, various methods have been reported for the simultaneous quantitation of two metal ions in solution [6,8–10]. One widely cited method uses PAR in combination with two additional chelators, ethylenediaminetetraacetic acid (EDTA) and nitrilotriacetic acid (NTA), to sequentially spectroscopically silence metals allowing for their quantitation [9]. We investigate the accuracy of this method herein, identifying inaccuracies arising from the limited specificity of the chelators.

Building on these earlier spectrophotometric assays [6,8,9], we have developed a facile, reliable, accurate and precise method for the simultaneous quantification of Cu^{2+} and Zn^{2+} in solution. The multicomponent PAR assay described herein uses spectral decomposition software to deconvolute the absorbance contributions of different species in solution allowing for high accuracy and precision in metal quantitation. The assay data fitting method can sensitively distinguish the spectral signals of PAR with bound Cu^{2+} (PAR:Cu^{2+}) and PAR with bound Zn^{2+} (PAR_2:Zn^{2+}). We determine optimal assay solution conditions and highlight important experimental considerations for using the PAR assay to analyze metalloproteins. The assay methodology is general and may be applied to the study of many proteins binding various metal ion combinations (e.g. Ni^{2+} and Cu^{2+}, Ni^{2+} and Co^{2+}, Zn^{2+} and Co^{2+}).

We demonstrate the utility of the developed multicomponent PAR assay by using it to analyze the human metalloenzyme, Cu,Zn superoxide dismutase1 (SOD1). This widely studied model protein is implicated in causing the common and invariably fatal neurodegenerative disease amyotrophic lateral sclerosis (ALS) [16]. Many chemically and structurally diverse mutations in SOD1 contribute to onset of ALS [17], yet little is known about metal binding by these mutant proteins. Initial studies provide evidence for weakened affinity and selectivity of metal binding for some mutants [9,18–20] and for enhanced neurotoxic misfolding and aggregation of SOD1 in the absence of full or correct metal incorporation [21,22]. Metal binding has dramatic impacts on the structure, stability, activity and

dynamics of SOD1 [1,22,23], as for other proteins [1,2,24]. Thus, this paper illustrates the value of the multicomponent PAR assay approach for facile and accurate metal quantification of proteins.

2. Materials and Methods

2.1. Solutions

All solutions were prepared using Milli-Q ultrapure water (18.2 MΩ·cm; Millipore Ltd., Bedford, MA). which was confirmed by ICP-MS to have < 0.03 ppt Cu^{2+} and < 0.77 ppt Zn^{2+}. All glassware, pipette tips, Eppendorf tubes and cuvettes were washed with nitric acid (50% (v/v) followed by Milli-Q water to remove contaminating metals. Metal stock solutions (100 mM) of Cu^{2+} and Zn^{2+} were prepared by dissolving the appropriate amount of $CuSO_4 \cdot 5H_2O$ and $ZnCl_2$ in water using a volumetric flask. Working metal stock solutions (0.25 mM) were prepared volumetrically by further dilution with water. A guanidine hydrochloride (GdnHCl; $CH_5N_3 \cdot HCl$) stock solution (8 M) was prepared by dissolving the denaturant in water to a final volume of 300 mL and determining the concentration by refractive index [25]. Stock solutions (80 mM) of ethylenediaminetetraacetic acid (EDTA; $C_{10}H_{14}N_2O_8Na_2 \cdot 2H_2O$) and nitrilotriacetic acid (NTA; $C_6H_9NO_6$) were prepared by dissolving the appropriate amount of chelator in water. Sodium hydroxide (NaOH; 16mM) was added to the NTA solution.

A stock solution of PAR (10 mM) was prepared by dissolving the chelator (Sigma Aldrich; 98% purity) in water. Working 4x PAR stock solutions were prepared by combining the appropriate amount of the PAR stock solution (final sample PAR concentration of 100 µM unless otherwise stated) with 2.12 g of 4-(2-hydroxyethyl)-1-piperazineethanesulfonic acid (HEPES; $C_8H_{18}N_2O_4S$) and water to a final volume of 40 mL. The pH of the 4x PAR solution was adjusted to 8.0 using 1 M NaOH. A final assay volume of 500 µL was comprised of 1x PAR, 5.4 M GdnHCl, and 50 µL of the solution being analyzed (which may be a protein solution or a stock metal) and was measured to have a pH of 8.2 with a standard electrode. As PAR deteriorates when exposed to light and in glass bottles, all PAR solutions were stored in plastic conical vials covered in aluminum foil at 4°C to minimize degradation.

2.2. Preparation and purification of recombinant SOD1

All variants of SOD1 are in the pseudo wild-type (pWT) background, a variant of SOD1 in which the two free cysteines at position 6 and 111 have been mutated to alanine and serine, respectively, to prevent formation of aberrant intermolecular disulfide bonds. pWT has been characterized extensively and exhibits essentially the same stability, enzymatic activity and structure as WT SOD1 [19,22,23]. Recombinant pWT and mutant SOD1s were expressed as described previously using shaker flask cultures [26,27] or fed-batch fermentation [28]. In the expression system used, SOD1 is exported to the periplasm from which it is obtained by osmotic shock for shaker flask cultures, or from the culture supernatant of fermentation cultures using ammonium sulfate (40% w/v) precipitation. Then SOD1 variants were purified using a modification of the procedure of Getzoff *et al.* with Poros HP2 hydrophobic interaction chromatography replacing the diethylaminoethyl chromatography. The SOD1

concentration was determined by absorbance using the extinction coefficient at 280 nm, ε_{280} = 5, 400 M^{-1} cm^{-1} [29].

2.3. Sample preparation and measurement

For metal determination, 450 µL of the 1x PAR solution was mixed with 50 µL of sample solution containing the desired concentration of metal (Cu^{2+}, Zn^{2+} or both). For protein metal determination, the protein (50 µL) was first added to GdnHCl (337.5 µL) and incubated for 40 minutes to allow sufficient time for the protein to unfold. Then the 4x PAR solution was added (112.5 µL) and the sample was thoroughly mixed using a micropipette. The final assay solution conditions were 100 µM PAR, 50 mM HEPES (pH 8.2) and 5.4 M GdnHCl, unless otherwise stated. In all cases, absorbance scans were measured from 200 nm to 800 nm at room temperature on a Cary 300 UV-Visible spectrometer (Agilent Technologies) using a cuvette with a 1 cm pathlength. Throughout the paper, replicate measurements refer to measurements of multiple samples within one experiment.

The preparation and measurement of samples for metal determination using the Crow method were performed as described in Crow *et al.,* 1997 [9] with the exceptions that HEPES buffer (50 mM) was used instead of sodium borate buffer (100 mM) and the final sample pH was 8.2 instead of 7.8. Trace background metals were accounted for by subtracting observed decreases in absorbance at 500 nm upon the addition of NTA and EDTA in the absence of added metal. Dilution upon the addition of EDTA and NTA was not accounted for as the effect on calculated metal content was minimal (≤ 1.5%).

2.4. Spectral fitting method (SpLab)

For metal quantitation using the multicomponent PAR assay, the spectral decomposition software SpectraLab or SpLab (created by Dmitri Davydov, Washington State University, [30]) was used to determine the absorbance contributions of different species in solution (Figure A.1). SpLab is freely available for download (http://cyp3a4.chem.wsu.edu/spectralab.html). With SpLab, spectral decomposition is achieved using the linear least squares method to minimize the sum of the squared deviations (residuals) between the observed absorbance and the fitted value. Using this software, the experimental spectrum is fit as a linear combination of three absorbance standards: free PAR, PAR:Cu^{2+} and PAR_2:Zn^{2+}. The concentration of each metal in the sample is calculated from the fraction of each standard spectrum in the fitted spectrum, which is determined from the weighting coefficient in the SpLab output.

For the multicomponent PAR assay, the experimental absorbance spectrum of the sample, *A,* is fit as:

$$A = Component_1 + Component_2 + Component_3 \qquad Eq.1$$

where $Component_i = w_i$ x $Standard_i$. The w_i and $Standard_i$ correspond to the weighting coefficient and standard spectrum for component i, respectively, and $Standard_1$, $Standard_2$ and $Standard_3$ are the spectra for 100 µM PAR, 10 µM Cu^{2+} in 100 µM PAR, and 10 µM Zn^{2+} in 100 µM PAR, respectively. The concentration of Zn^{2+} (or Cu^{2+}) in the sample is given by wi x 10 µM.

Additional details for using SpLab are given in the legend of Figure A.1. Note that principal component analysis is also available in SpLab and can be used for spectral deconvolution. However, for lower metal concentrations or noisy spectra using the abovementioned fitting routine with a set of standard spectra gives more accurate and reliable results

2.5. Analysis of the accuracy and precision of the PAR Assay

To test the accuracy of the PAR assay, samples of known concentrations of free Cu^{2+} and Zn^{2+} were analyzed, comparing the agreement between the expected and calculated values for each metal. In addition, the metal content of protein samples analyzed by ICP-AES and the PAR assay were compared. ICP-AES is a sensitive metal quantitation method with a detection limit < 1 ppb. Protein samples (0.3 mM to 0.5 mM; 300 µL) were diluted to 3 mL using Milli-Q water prior to analysis by ICP-AES. The precision of the PAR assay was assessed by measuring the average and standard deviation for samples prepared in triplicate (unless otherwise stated).

2.6. Differential scanning calorimetry

Differential scanning calorimetry (DSC) of SOD1 was performed to assess protein stability and metalation as described previously [27,31,32], using a LLC VP-DSC instrument (MicroCal Inc., Malvern Instruments Ltd.). SOD1 samples (0.2 – 1.0 mg mL^{-1}) were buffered in 20 mM HEPES at pH 7.8. Buffer/buffer baselines were determined for each experiment and subtracted from protein/buffer scans. Data were normalized for protein concentration. Experiments used a scan rate of 1 °C min^{-1}.

3. Results and Discussion

3.1. Extinction coefficients

The free PAR absorption spectrum exhibits a symmetric peak with a maximum absorption (λ_{max}) at 416 nm (Figure 1A). Upon metal binding, the absorbance at 416 nm decreases and a shoulder appears at approximately 500 nm. The λ_{max} and shape of the shoulder are dependent upon the identity of the bound metal (Figure 1A). The molar extinction coefficients of the PAR:Cu^{2+} and PAR_2:Zn^{2+} complexes, calculated from the slopes of Cu^{2+} and Zn^{2+} standard curves at 500 nm (Figure 1B), are 36,167 $M^{-1}cm^{-1}$ and 75,225 $M^{-1}cm^{-1}$, respectively. This measured Cu^{2+} extinction coefficient closely matches the previously reported value [9]. The extinction coefficient for Zn^{2+} is comparable to values reported previously [6,9,33]; we note though that this extinction coefficient is sensitive to solution conditions such as pH [9,33] and the binding stoichiometry of PAR and Zn^{2+}, which can switch from 2:1 to 1:1 under certain solution conditions (see 3.2.). Fitting the absorption spectra of various combinations of Cu^{2+} and Zn^{2+} with PAR (Figure 1C) demonstrates that the observed spectra correspond to a linear combination of the free PAR, PAR:Cu^{2+}, and PAR_2:Zn^{2+} spectra, which can be leveraged to simultaneously quantitate two metal ions in solution, described below.

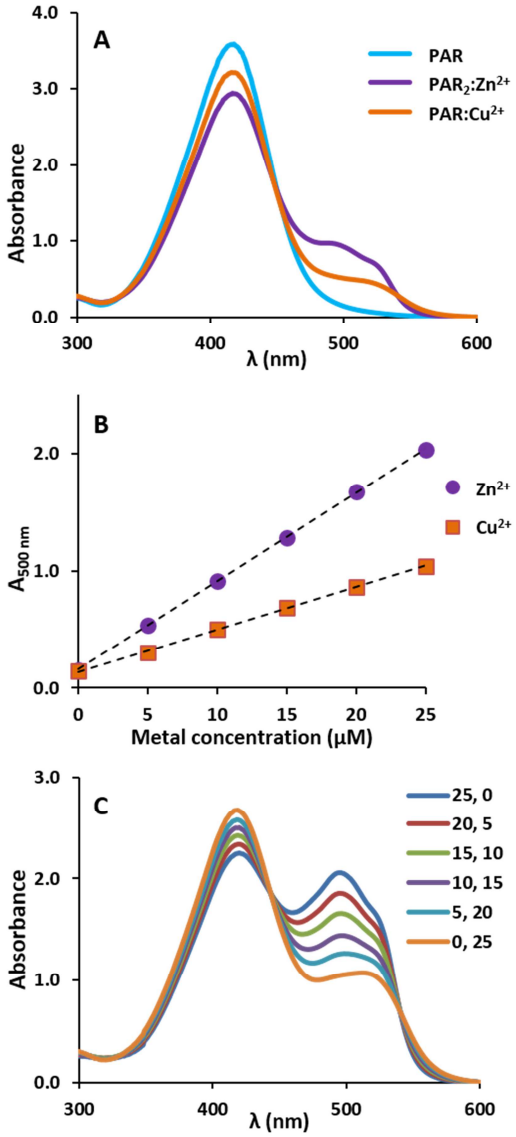

Figure 1. Representative absorption spectra and standard curves of Cu^{2+} and Zn^{2+} for the PAR assay. (A) Absorption spectra of 100 μM PAR in the absence of added metal and with addition of 10 μM Cu^{2+} or Zn^{2+}. (B) Standard curves of Cu^{2+} and Zn^{2+} at 500 nm. Extinction coefficients corresponding to the slopes of the lines determined by linear regression are 75,225 M^{-1} cm^{-1} and 36,167 M^{-1} cm^{-1} for Zn^{2+} and Cu^{2+}, respectively. (C) Experimental spectra for samples of known mixtures of Cu^{2+} and Zn^{2+} in 100 μM PAR with the total metal concentration equal to 25 μM. The concentration of each metal is given in the legend as Zn^{2+}, Cu^{2+} (μM).

3.2. Optimization of assay solution conditions

In developing the multicomponent PAR assay, we first considered the optimal PAR concentration to use. Previous metal quantitation assays using PAR have the chromogenic chelator concentration in the range of 50 to 100 μM [6,8,9]. When deciding what concentration of PAR to use it is important to consider the effect of the chelator concentration on the stoichiometry of metal binding. Previous investigations suggest that PAR and Zn^{2+} form 2:1 complexes only when free PAR is in at least

2.5-fold molar excess over Zn^{2+} [9]. This is illustrated by analysis of Zn^{2+} standard curves at 50 µM and 100 µM PAR (Figure 2A). When the PAR concentration is 50 µM, there is a clear deviation from linearity at Zn^{2+} concentrations of 15 µM and higher, indicative of a change in the binding stoichiometry once PAR is no longer in 2.5-fold molar excess. When the PAR concentration is 100 µM, the curve remains linear at all Zn^{2+} concentrations studied, up to 25 µM Zn^{2+}. On the other hand, PAR and Cu^{2+} appear to form a 1:1 complex at both 50 and 100 µM PAR, as evidenced by the high degree of linearity for both standard curves (Figure 2B). Based on these results, the concentration of PAR used herein was chosen to be 100 µM with the total metal concentration in samples not exceeding 25 µM to avoid changes in the binding stoichiometry of PAR and Zn^{2+} and to therefore stay within the range of linearity.

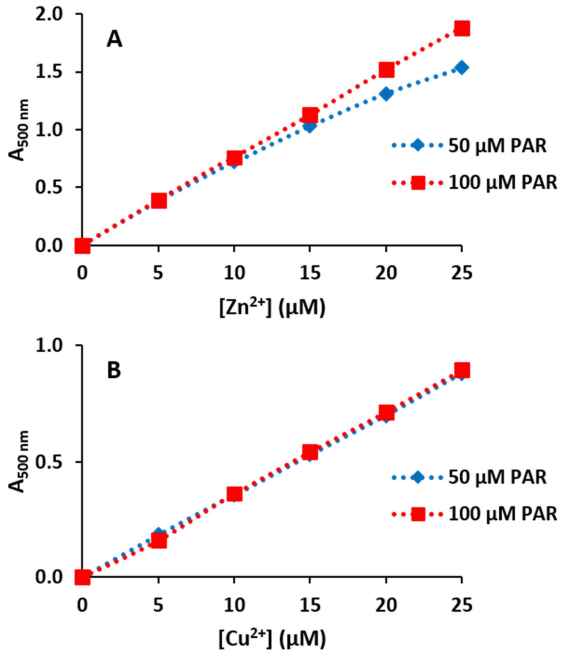

Figure 2. Metal standard curves in 50 µM and 100 µM PAR. (A) Zn^{2+} standard curve (0 – 25 µM). In the 50 µM PAR condition, there is a clear deviation from linearity indicative of a change in the binding stoichiometry of PAR and Zn^{2+} once PAR is not in sufficient excess relative to Zn^{2+}. (B) Cu^{2+} standard curve (0 – 25 µM). Plotted values are for measurements of a single sample. The Cu^{2+} standard curve remains linear at all Cu^{2+} concentrations studied in both the 50 µM and 100 µM PAR condition. In panels A and B data are offset to zero absorbance for zero added metal. The dotted lines are to guide the eye and correspond to interpolated data values.

3.3. Fitting with SpLab: Standard spectra

As described earlier, the unique spectral properties of different metals complexed with PAR can be exploited to simultaneously quantitate two metals in solution [6,8]. With SpLab, spectral decomposition is achieved using the linear least squares fitting method. Using this software, an experimental spectrum was fit by a set of three standard spectra representing the three absorbing species in solution: free PAR, PAR:Cu^{2+} and PAR_2:Zn^{2+} (Figure 1A). The concentration of the PAR absorption standard used for fitting is 100 µM, representative of the spectrum for PAR prior to the

addition of metal. Suitable concentrations for the PAR:Cu^{2+} and PAR_2:Zn^{2+} standard spectra were determined by fitting samples of known metal concentrations with standards having concentrations ranging from 5 – 25 µM. This represents the range where the change in absorbance is large but accurately measurable and is proportional (i.e. linear) to the amount of metal in solution (see above). From analyzing both the correspondence to expected values and standard deviation between multiple samples within one experiment, we found that fits using absorption standards of 10 µM Cu^{2+} and 10 µM Zn^{2+} gave the most accurate values with the lowest uncertainties. The final fitted spectrum is a linear combination of the three component spectra (Figure 3). The component spectra correspond to the PAR, PAR:Cu^{2+} and PAR_2:Zn^{2+} standard spectra each multiplied by a weighting coefficient. The concentration of each metal ion in solution is obtained by multiplying the weighting coefficient for the corresponding component spectrum by the concentration of the original standard spectrum (see Figure 3 legend).

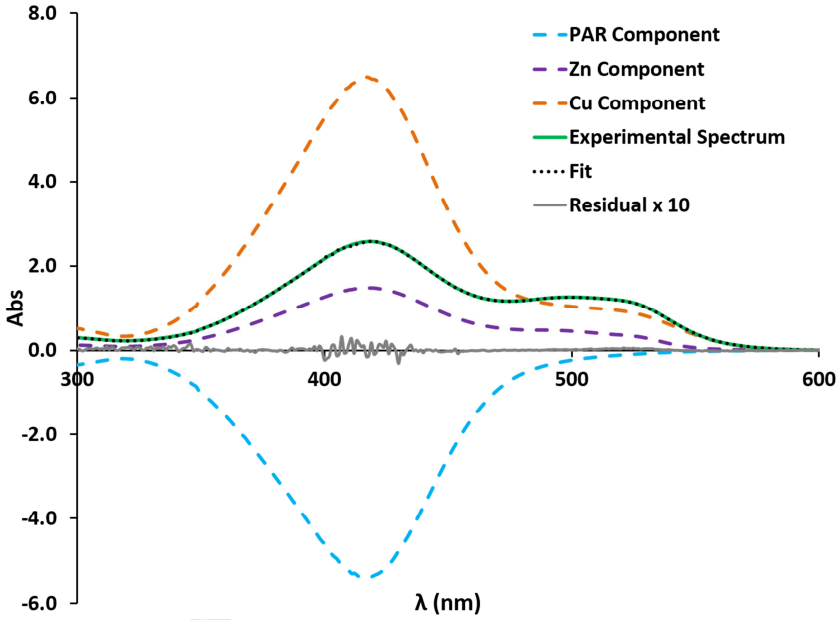

Figure 3. Example of multicomponent PAR assay analysis using SpLab. Experimental spectrum (solid green line) of sample containing 20 µM Cu^{2+} and 5 µM Zn^{2+} and the three fitted components determined by SpLab (dashed lines) sum to the fitted spectrum (black dotted line) which very closely matches the experimental spectrum (r^2 0.99).The very small residual between the experimental and fitted spectra is shown with 10-fold increased scale (solid grey line). Component spectra were calculated using the weighting coefficients determined from the fit of the experimental spectrum by the three standard spectra, illustrated in Figure 1A. The weighting coefficients of $component_1$ (PAR), $component_2$ (PAR:Cu^{2+}) and $component_3$ (PAR_2:Zn^{2+}) in the fitted spectrum are -1.5, 2.0 and 0.49, respectively. Thus, in this case the concentration of Cu^{2+} and Zn^{2+} are calculated to be 20.0 µM and 4.90 µM, respectively, in excellent agreement with the known concentrations.

3.4. Protein analysis: denaturation, sample measurement and concentration

Since many native proteins bind metals with high affinity (e.g. for SOD1, K_d for Cu^{2+} and Zn^{2+} are estimated as < 10^{-18} M and 10^{-14} M, respectively [9,34]), proteins should be unfolded during the PAR assay to ensure quantitative metal release by the protein and complete binding of the metals by PAR.

The time required for unfolding depends on the strength of the denaturant as well as the stability of the protein. Two chemical denaturants commonly used to unfold proteins are urea and GdnHCl. For time efficiency, and to ensure that even very stable proteins can be assayed using this method, the PAR assay described herein uses the stronger denaturant, GdnHCl [35]. Under these assay conditions (8 M GdnHCl), even extremely stable proteins may be fully unfolded; for example, fully metalled SOD1, which has a melting temperature of approximately 92°C, will globally unfold within 40 minutes [31]. As SOD1 unfolds particularly slowly [19,36], this timeframe is likely to be sufficient to fully unfold most proteins [19]. To ensure complete unfolding for even more stable proteins, longer times and/or higher concentrations of GdnHCl could be used (noting that the logarithm of the rate constants of unfolding generally increases linearly with denaturant concentration [35]).

Another important consideration for the success of this assay is the stability of PAR in solution, as it has been shown that PAR is sensitive to light [37]. Previously reported methods call for successive scanning of the sample to monitor changes in absorption as a function of time [8,9]. To investigate the effect of such scanning, we measured the absorbance (200-800 nm) of PAR_2:Zn^{2+} (100 µM:10 µM) for 5 successive scans (each scan ~40 s). After 5 scans the absorbance of PAR_2:Zn^{2+} at λ_{max} (495 nm) decreases by 0.01 Abs units, which corresponds to approximately 0.15 µM Zn^{2+} (or 1.5% of the total Zn^{2+}). While this value is relatively small, continued scanning for longer times or for samples with lower metal concentrations would increase the error. Based on these results, and to avoid photodamage of the PAR, we suggest that proteins first be incubated in GdnHCl for 40 min to allow for complete unfolding before adding PAR. After unfolding, the protein/GdnHCl solution should be mixed with the 4x PAR solution just prior to sample measurement. Previous studies have shown that the binding of metals (e.g. Zn^{2+}) by PAR is rapid and usually complete within 2 to 3 ms, therefore a long incubation period with PAR is not necessary [13].

We also explored suitable protein concentration for the analysis. The protein concentration needs to be high enough to produce a measurable change in absorbance yet low enough to satisfy the constraint that the amount of free PAR be in at least 2.5 molar ratio relative to the total metal in solution (Figure 2). Also, remembering that PAR binds Zn^{2+} with a 2:1 stoichiometry, Zn^{2+} will remove twice as much free PAR as Cu^{2+}. In the case of SOD1, which binds one Cu^{2+} and one Zn^{2+} ion per monomer, protein concentrations ranging from 1 to 9 µM (SOD1 monomer) will satisfy these constraints (assuming SOD1 is fully metallated and a starting concentration of 100 µM PAR). Protein concentrations within this range were tested and had very little effect on the accuracy and precision of the assay, defining a suitable protein concentration range for the assay. For further experiments described below, a final protein concentration of 5 µM was used.

3.5. Determination of the accuracy and precision of the SpLab PAR Assay

To assess the accuracy and the precision of the multicomponent PAR assay, a variety of samples, without and with protein (5 µM), containing known amounts of Cu^{2+} and Zn^{2+} were tested. Analysis of samples with varying amounts of Cu^{2+} and Zn^{2+} in the absence of protein are given in Table 1. In every case the expected and calculated metal concentrations are within 5%, and, the standard deviation is generally ≤ 3%. These results demonstrate that the multicomponent PAR assay can be used to

deconvolute the spectral signals of the three absorbing species in solution with high accuracy and precision. Samples containing increasing concentrations of individual metals were also tested to ensure that the data could be fit accurately in the absence of the other metal and showed excellent agreement between known and measured concentrations (Figure A.2 and Table A.1).

Table 1. Accuracy and precision of the simultaneous determination of Cu^{2+} and Zn^{2+} in solution using the multicomponent PAR assay

Added concentration (μM)		Calculated concentration (μM)		Calculated % metal	
Cu^{2+}	Zn^{2+}	Cu^{2+}	Zn^{2+}	Cu^{2+}	Zn^{2+}
0.0	25.0	0.2 ± 0.2	24.9 ± 0.3	-	99 ± 1
5.0	20.0	4.9 ± 0.3	20.9 ± 0.5	98 ± 7	104 ± 2
10.0	15.0	9.7 ± 0.3	15.3 ± 0.1	97 ± 3	102 ± 1
15.0	10.0	15.1 ± 0.3	10.2 ± 0.0	101 ± 2	102 ± 0
20.0	5.0	20.3 ± 0.1	5.1 ± 0.0	101 ± 1	101 ± 0
25.0	0.0	24.9 ± 0.4	0.0 ± 0.1	99 ± 2	-

Each value represents the mean ± the standard deviation of measurements on three replicate samples within one experiment. The percent (%) metal was calculated as ([calculated metal] / [known metal])*100%.

We also assessed the accuracy and precision of this assay in the presence of protein to ensure that protein does not interfere with the results. As an independent measure of metal content, ICP-AES was used to determine the metal content of two SOD1 variants with distinctly different metalation properties, pWT and the ALS-associated mutant, H46R. H46 coordinates bound Cu^{2+} in pWT and upon its mutation to R the protein is unable to bind Cu^{2+} at the native Cu^{2+} site [38]. H46R has decreased thermal stability compared to pWT and one of the longest disease durations among all ALS-associated mutations [39,40]. The results show that the metal concentrations determined using ICP-AES and the PAR assay for pWT and H46R are in excellent agreement (Table 2). This provides further evidence that the PAR assay described herein can quantitate the metal ion content of metalloproteins with high accuracy.

Table 2. Metalation of SOD1 measured by multicomponent PAR assay and ICP-AES

	PAR		ICP-AES		Difference	
SOD1 sample	Cu^{2+}	Zn^{2+}	Cu^{2+}	Zn^{2+}	Cu^{2+}	Zn^{2+}
pWT	0.82 ± 0.01	1.11 ± 0.02	0.82	1.08	0.00	0.03
H46R	0.0 ± 0.0	1.04 ± 0.03	0.02	1.11	0.02	0.06

All SOD1 samples were purified from fermenter cell cultures (see 2.2s, with no exposure to EDTA (see 3.7). SOD1 concentrations for PAR assay were 5 μM monomer. For ICP-AES, 3 mL of 30 μM monomer protein was analyzed (see Methods). Values are calculated as fraction metal per protein subunit, where full metalation corresponds to 1.00. The differences are calculated as the absolute value of fraction metal PAR - fraction metal ICP-AES. The two methods are in very close agreement. ICP-AES analysis was completed at the Analytical Laboratory for Environmental Science Research and Training, University of Toronto, Toronto, Ontario, Canada.

3.6. Analysis of previous PAR assay method for metal quantification

For comparison, we also investigated the accuracy and precision of a previously reported, extensively cited PAR assay methodology [9]. The PAR assay protocol developed by Crow *et al*. employs two chelators, NTA and EDTA. In this assay, PAR is used to bind Cu and Zn released by SOD1 unfolded in GdnHCl. Next, NTA is added with the associated change in A_{500} attributed to the quantitative removal of Zn from PAR by the NTA . A further change in A_{500} occurs with the subsequent addition of EDTA and is attributed to the quantitative removal of Cu from PAR by EDTA. Thus, this method assumes specific removal from PAR of Zn^{2+} by NTA and of Cu^{2+} by EDTA.

We tested the accuracy and precision of this method by analyzing samples with known combinations of Cu^{2+} and Zn^{2+}. The results reveal significant errors for a range of sample conditions (Table A.2). For example, when the concentration of Zn^{2+} is 4-fold greater than the concentration of Cu^{2+}, the error especially for Cu^{2+}, is largest (215% compared to the expected 100%). When the concentration of Zn^{2+} is smaller than Cu^{2+} or the concentrations of both metals are equal, the error is reduced but still significant (88-128%). In almost every case the multicomponent PAR assay described herein gives significantly lower error than that observed for the Crow methodology (Figure 4).

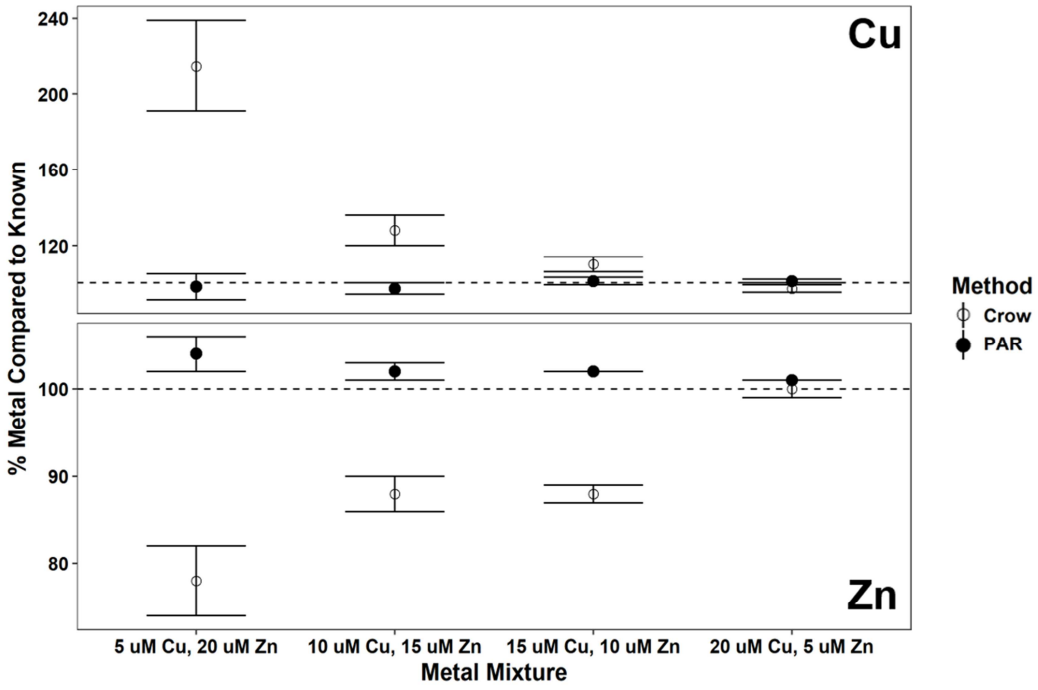

Figure 4. Comparison of the accuracy of the Crow and multicomponent PAR assay methods. The symbols for the different methods are given in the legend. The known concentrations of each metal in the sample are given on the x-axis as Cu^{2+}, Zn^{2+} (μM). The % metal compared to known was calculated as ([calculated metal]/[known metal]) * 100% for Cu^{2+} (upper panel) and Zn^{2+} (lower panel). The points are the mean value for measurements of 3 or 2 independent samples (PAR and Crow, respectively) with error bars representing 1 SD. Raw data are in Table 1 (PAR) and Table A.2 (Crow).

To identify the source of error in the Crow methodology, we investigated the specificities of the chelators NTA and EDTA for binding the respective target metals by measuring the associated spectral changes (Figure 5). The results show that NTA and EDTA do not quantitatively strip Zn^{2+} and Cu^{2+}, respectively, from PAR. For example, for 20 µM Zn^{2+}, NTA does not chelate all of the Zn^{2+} present (Figure 2A). In fact, even though NTA is in 40-fold excess over Zn^{2+} and 8-fold excess over PAR, the chelator binds just 93% of the Zn^{2+}; the remaining 7% of Zn^{2+} is removed from PAR by the addition of 0.8 mM EDTA. Furthermore, for 20 µM Cu^{2+}, there is a small, but clear decrease in absorbance upon the addition of NTA, indicating that the chelator is removing approximately 5% of the Cu^{2+} from PAR (Figure 2B). These experiments were repeated at 3 different Cu^{2+} and Zn^{2+} concentrations (5, 10 and 15 µM) with the same trend being observed (data not shown).

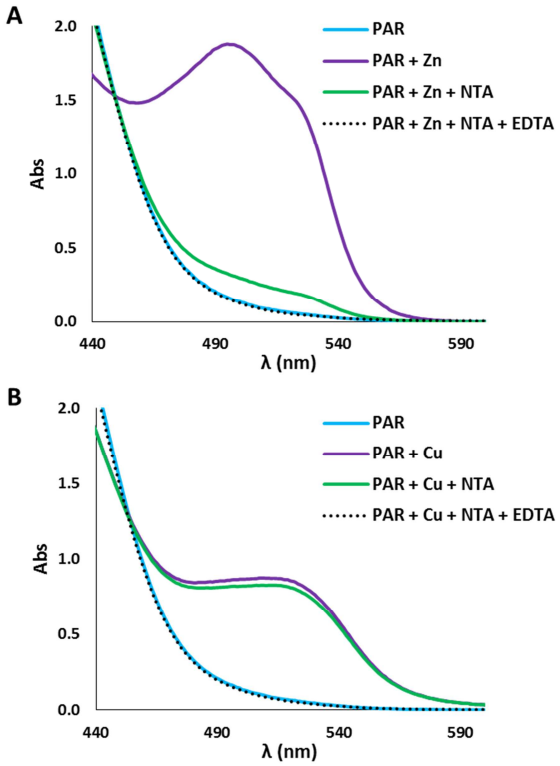

Figure 5. Specificity of the chelators used in previous PAR assay for simultaneous Cu^{2+} and Zn^{2+} determination. In this assay, the decrease in absorbance at 500nm (ΔAbs_{500}) is converted to the concentration of metal bound by each chelator using Beer-Lambert's law and the corresponding extinction coefficient [9]. (A) Changes in the absorption spectrum of PAR (100 µM) with Zn^{2+} (20 µM) (purple), upon addition of NTA (0.8 mM) (green) followed by EDTA (0.8 mM) (dotted line).The spectral change upon addition of NTA corresponds to removal of 93% of the 20 µM Zn^{2+} from PAR, while EDTA addition removes the remaining 7%. (B) Changes in the absorption spectrum of PAR (100 µM) with Cu^{2+} (20 µM), upon addition of NTA (0.8 mM) and then EDTA (0.8 mM). The absorbance change upon addition of NTA corresponds to removal of 5% of the Cu^{2+} from PAR, with EDTA removing the remaining Cu^{2+}.

The results of the spectral changes for mixtures of PAR, NTA and EDTA (Figure 5) help explain the observed trends in the errors associated with the Crow method (Table A.2 and Figure 4). For example, as mentioned earlier, when the concentration of Zn^{2+} is greater than that of Cu^{2+}, the error,

especially for Cu^{2+}, is largest. This is because when the concentration of Zn^{2+} is high, NTA does not bind all of the Zn^{2+} present leaving the remaining Zn^{2+} to be bound by EDTA. This results in a higher than expected Cu^{2+} value and a lower than expected Zn^{2+} value. The error in the Cu^{2+} value is further amplified by the fact that the extinction coefficient for the PAR:Cu^{2+} complex is nearly half that of PAR_2:Zn^{2+}, and therefore any Zn^{2+} misattributed to Cu^{2+} is "counted" approximately twice. On the other hand, when the concentration of Zn^{2+} is low relative to Cu^{2+}, NTA will bind some Cu^{2+} resulting in a lower than expected Cu^{2+} measurement and a higher than expected Zn^{2+} measurement. When the concentration of both metals in solution is equal the calculated metal content is more accurate, although generally some of the Zn^{2+} is still misattributed to Cu^{2+}. Overall, the results show that the type and amount of metal bound by NTA is dependent upon the relative concentration of each metal in solution. Thus, lack of full specificity by the chelators helps explain the larger errors associated with the Crow method compared to the multicomponent PAR assay described herein (Figure 4).

3.7. Application of multicomponent PAR assay: metalation of disease-associated SOD1 mutants

Using the multicomponent PAR assay, we investigated the metalation of pWT SOD1 and 9 ALS-associated mutants. The results indicate that all the proteins appear to be undermetallated (Table 3). On average, SOD1 variants contain 0.72 (± 0.18) Zn^{2+} equivalents/monomer and 0.62 (± 0.18) Cu^{2+} equivalents/monomer. This result is notable because pWT has extremely high affinity for Cu^{2+} and Zn^{2+} (estimated as > 10^{-18}M and 10^{-14}M, respectively [9]), and while mutants may have altered metal binding, many have very high activity and stability, which depend on metal binding [9,20,29,34,41]. Measurements of SOD1 variants' stability by differential scanning calorimetry (DSC) (Table 3), which is a sensitive reporter of metal binding [31,32], indicates that these samples have higher metalation levels than indicated by the PAR assay. For example, based on the PAR assay pWT has 0.78 Cu^{2+} equivalents/monomer and 0.89 Zn^{2+} equivalents/monomer, yet it has a T_m of 91.4°C (Table 3), which is comparable to that of fully metallated pWT (92°C) [31]. The presence of protein does not interfere with the accuracy or precision of the PAR assay (Table 2), thus the systematically low metalation values for these samples must be due to another source of error.

Table 3. Metal-ion content determined by multicomponent PAR assay and stability of pWT and 9 ALS-associated SOD1 mutants

SOD1 Variant	Cu^{2+}/monomer	Zn^{2+}/monomer	T_m (°C)
pWT	0.78 ± 0.01	0.89 ± 0.00	91.41
A4S	0.72 ± 0.06	0.75 ± 0.05	88.35
A4V	0.62 ± 0.00	0.74 ± 0.00	86.73
G41D	0.62 ± 0.03	0.76 ± 0.04	85.74
G41S	0.65 ± 0.06	0.77 ± 0.05	82.64
H43R	0.58 ± 0.03	0.76 ± 0.03	85.82
G85R	0.47 ± 0.03	0.58 ± 0.01	77.46
G93A	0.66 ± 0.04	0.80 ± 0.05	87.53
E100K	0.84 ± 0.05	0.78 ± 0.03	89.01
V148I	0.67 ± 0.01	0.85 ± 0.01	93.07

All SOD1 samples were prepared from shaker flask cell cultures, with exposure to EDTA during initial osmotic shock. Metal values are given as average equivalents per monomer ± the standard deviation of measurements of three independent samples in one experiment (except A4V which the average of is two independent samples). Full metal incorporation is 1 equivalent per monomer. The temperature where half of the protein is unfolded, or *Tm*, was measured by DSC.

Further investigation showed that these results are related to the presence of EDTA bound to the SOD1, which partially masks the metal ions. During the preparation of these SOD1 variants from E. coli grown in shaker flasks, EDTA is required in an initial osmotic shock step to ensure release of the SOD1 protein from the periplasm [26,32]. EDTA is not used in any of the following purification steps, including heat treatment, chromatography, and extensive dialysis. Nevertheless, EDTA is known to bind with high affinity to SOD1 [42] and it appears still to be bound to the final sample based on the systematically low PAR assay results here (Table 3). This conclusion is supported by size-exclusion chromatography experiments for SOD1 prepared from shaker flask cultures which exhibit a small characteristic EDTA peak. As EDTA is commonly added to many buffers to chelate metals and reduce protein damage caused by metalloproteases, these results highlight that care should be taken to avoid the presence of EDTA when using PAR assays.

To confirm that the metalation values in Table 3 obtained using the multicomponent PAR assay are indeed erroneously low, we again used ICP-AES to obtain an independent measure of metal content for a pWT SOD1 sample (Table 4). It should be noted that the samples initially assessed by ICP-AES (~~Table 2~~) were prepared from *E. coli* cells grown in a fermenter, where~~in~~ the SOD1 is naturally released from the periplasm and no use of EDTA in an osmotic shock step is required; thus, this SOD1 protein is never exposed to EDTA during purification *(Table 2)*. Indeed, the metalation values for these samples determined by both methods are in excellent agreement, showing the protein does not interfere with the PAR assay. However, for protein samples prepared from cells grown in shaker flasks with exposure to EDTA, the metal ion content determined by PAR is approximately 20% lower than that determined by ICP-AES (Table 4).

Taken together, these findings suggest that EDTA does in fact remain bound to SOD1 samples prepared using a typical shaker flask cell growth, and that the bound EDTA will mask a proportion of the metal present resulting in falsely low numbers. The presence of protein-bound EDTA would also interfere with any of the PAR assay methodologies described previously [6,8,9,15]. The results here point out an important potential source of error in this type of methodology which may be commonly overlooked. While the presence of EDTA does interfere with the assay, if we assume the amount of bound EDTA is relatively constant (as a single stock EDTA solution was prepared and used in the same way in osmotic shock during the preparation of all proteins), the results show that in general SOD1 mutants tend to have overall lower metalation levels than the pWT. Notably, the metal ion content is lowest for the G85R mutant, consistent with its demonstrated markedly weakened metal binding compared to the other mutants, which are all considered to be wild-type like with respect to metal binding and activity [34]. Also, A4V was suggested to have somewhat decreased Zn affinity [9]. Taken together, these results suggest that various SOD1 mutations tend to interfere with proper metalation.

Table 4. Metal content of pWT SOD1 from shaker flask cultures by multicomponent PAR assay and ICP-AES

Method	Cu^{2+}	Zn^{2+}
PAR	0.70	0.82
ICP-AES	0.89	1.08
Difference	**0.18**	**0.25**

Values are calculated as fraction metal per protein subunit, where full metalation corresponds to 1.00. The differences are determined to be the absolute value from the subtraction of the metal concentration determined by ICP-AES from that determined by the PAR assay. It should be noted that the pWT sample used here was obtained from a different preparation than that in Table 3. ICP-AES analysis was performed at Solutions Analytical Laboratory, University of Waterloo, Waterloo, Ontario, Canada.

3.8. Considerations for using a spectrophotometric chelator for metal quantitation and other applications

Use of a spectrophotometric chelator for metal quantitation provides the advantages of low cost, high sensitivity and a small time requirement; there are, however, some additional potential issues to using PAR that should be addressed. As previously mentioned, PAR is light sensitive [37]. Thus, it is important to ensure proper storage of PAR solutions and avoid methodologies that involve prolonged light exposure to avoid degradation of PAR. PAR has also been shown to deteriorate significantly over short periods of time when stored in glass bottles, regardless of the extent of light exposure [37]. We have found that when stored in plastic conical vials in the dark at 4°C, PAR solutions (100 µM or 10 mM) can last up to a year with little degradation. Therefore, PAR is relatively stable under suitable conditions.

The possibility of contaminating metal-binding species must also be considered when using the PAR assay. An example of this is found in Section 3.7 wherein previously unidentified protein-bound EDTA proved to be an issue in analysis of SOD1 samples. Any contaminating species with affinity for the metals in question present a potential source of error. Insufficiently unfolded protein may also act as a

contaminating species: buried, protein-bound metals are less likely to be bound by the PAR, interfering with the assay. Since the unfolding rate of proteins generally has a logarithmic dependence on the GdnHCl concentration, for extremely stable proteins a higher concentration of the denaturant may be needed to successfully overcome this consideration.

The method described herein may be adaptable to a variety of applications. For example, colorimetric methods are commonly employed for automated and high-throughput analysis. To be suitable for high-throughput measurements, the assay should ideally be fast and low cost, sensitive so that minimal sample is required, in a format to facilitate measuring large numbers of samples, and preferably use common, easily-accessible lab equipment, such as a spectrophotometer. Thus, Hogbom and coworkers developed a high-throughput, multi-step, luminol/PAR assay for metal detection and single metal identification in 384-well plates, suitable for proteomics applications [15]. While the PAR assay described herein is not applicable to complex biological samples containing many different proteins and metals in low amounts, it could be useful for the rapid measurement of large numbers of samples as it has relatively low protein requirements (e.g. ~5 µM SOD1 monomer at 500 µL here, or ~100 µL in plates, ~40 – 8 µg), can be completed in under an hour, and may be optimized for a multi-well plate format. We caution that care should be taken for such applications to ensure sufficient signal in smaller sample volume wells to accurately measure the different metals. Also, the PAR method may be extendable to other combinations of metals, such as Ni^{2+} and Cu^{2+}, Ni^{2+} and Co^{2+}, and Zn^{2+} and Co^{2+} for which PAR complexes exhibit spectral differences comparable in magnitude to those for Cu^{2+} and Zn^{2+} employed herein [6,14,33]. Diverse proteins, from enzymes to chaperones and structural proteins containing metals bound as individual ions or in clusters, may be amenable to analysis with the PAR method, when suitably denatured as described here in 8M GdnHCl to release metal. Thus, the method developed here may be valuable for a range of analyses for purified proteins.

4. Conclusions

We report herein a spectrophotometric method for the simultaneous quantification of multiple bound metals in proteins using the chromogenic chelator PAR. This method provides the advantages of being sensitive, facile, and low cost. Its application to the quantification of Cu^{2+} and Zn^{2+} in the metalloprotein SOD1 yielded a comparable accuracy to ICP-AES. This multicomponent PAR assay uses the spectral software SpLab [30] to perform spectral decomposition based on the signals of the three absorbing species in solution (PAR, PAR:Cu^{2+} and PAR_2:Zn^{2+}). Analysis simply requires the input of three standard absorption spectra at one set of solution conditions. The SpLab software is freely available and easily applied; other data fitting routines for similar or principal component analysis could alternatively be used, such as MS Excel or MATLAB. The developed method is versatile as changes to the experimental conditions can be simply accounted for in the standard spectra used for data fitting. Thus, the methodology is adaptable to other buffers, sample concentrations, or metals with distinguishable spectral signatures. In conclusion, the multicomponent PAR methodology developed here provides numerous attractive features that may be widely applied for protein metal content analysis.

Appendix

Figure A.1: SpLab software screenshot.

Figure A.2 Quantification of a Single Metal Species with PAR

Figure A.3. Specificity of the chelators used in previous PAR assay for simultaneous Cu^{2+} and Zn^{2+} determination.

Table A.1. Quantification of a Single Metal Species: Determination of Cu2+ and Zn2+ in solution using PAR assay protocol

Table A.2. Accuracy and precision of the simultaneous determination of Cu^{2+} and Zn^{2+} in solution using a previous PAR assay protocol.

References

[1] C.J. Wilson, D. Apiyo, P. Wittung-Stafshede, Role of cofactors in metalloprotein folding, Q Rev Biophys. 37 (2004) 285–314. doi:10.1017/S003358350500404X.

[2] T. Dudev, C. Lim, Metal binding affinity and selectivity in metalloproteins: insights from computational studies, Annu Rev Biophys. 37 (2008) 97–116. doi:10.1146/annurev.biophys.37.032807.125811.

[3] J.S. Garcia, C.S. De Magalhães, M.A.Z. Arruda, Trends in metal-binding and metalloprotein analysis, Talanta. 69 (2006) 1–15. doi:10.1016/j.talanta.2005.08.041.

[4] J. Szpunar, Biochemical speciation analysis by hyphenated techniques, Anal. Chim. Acta. 400 (1999) 321–332. doi:10.1016/S0003-2670(99)00628-5.

[5] A. Sanz-Medel, M. Montes-Bayón, M. Luisa Fernández Sánchez, Trace element speciation by ICP-MS in large biomolecules and its potential for proteomics, Anal. Bioanal. Chem. 377 (2003) 236–247. doi:10.1007/s00216-003-2082-z.

[6] C.E. Sabel, J.L. Shepherd, S. Siemann, A direct spectrophotometric method for the simultaneous determination of zinc and cobalt in metalloproteins using 4-(2-pyridylazo)resorcinol, Anal Biochem. 391 (2009) 74–76. doi:10.1016/j.ab.2009.05.007.

[7] C.E. Sabel, Investigations on the conformational stability and metal substitution of the Zn2+-dependent anthrax lethal factor protease and new strategies for the quantification of divalent metal ions in metalloproteins, Laurentian University, 2010.

[8] V.K. Mulligan, A. Kerman, S. Ho, A. Chakrabartty, Denaturational stress induces formation of zinc-deficient monomers of Cu,Zn superoxide dismutase: implications for pathogenesis in amyotrophic lateral sclerosis, J Mol Biol. 383 (2008) 424–436. doi:10.1016/j.jmb.2008.08.024.

[9] J.P. Crow, J.B. Sampson, Y. Zhuang, J.A. Thompson, J.S. Beckman, Decreased zinc affinity of amyotrophic lateral sclerosis-associated superoxide dismutase mutants leads to enhanced catalysis of tyrosine nitration by peroxynitrite, J Neurochem. 69 (1997) 1936–1944. doi:10.1046/j.1471-4159.1997.69051936.x.

[10] C.E. Säbel, J.M. Neureuther, S. Siemann, A spectrophotometric method for the determination of zinc, copper, and cobalt ions in metalloproteins using Zincon, Anal. Biochem. 397 (2010) 218–226. doi:10.1016/j.ab.2009.10.037.

[11] J.A. Platte, V.M. Marcy, Photometric Determination of Zinc with Zincon. Application to Water Containing Heavy Metals, Anal. Chem. 31 (1959) 1226–1228. doi:10.1021/ac60151a048.

[12] E. Hilario, I. Romero, H. Celis, Determination of the physicochemical constants and spectrophotometric characteristics of the metallochromic Zincon and its potential use in biological systems, J. Biochem. Biophys. Methods. 21 (1990) 197–207. doi:10.1016/0165-022X(90)90013-3.

[13] J.B. Hunt, S.H. Neece, A. Ginsburg, The use of 4-(2-pyridylazo)resorcinol in studies of zinc release from Escherichia coli aspartate transcarbamoylase, Anal Biochem. 146 (1985) 150–157. doi:10.1016/0003-2697(85)90409-9.

[14] K.A. McCall, C.A. Fierke, Colorimetric and fluorimetric assays to quantitate micromolar concentrations of transition metals, Anal Biochem. 284 (2000) 307–315. doi:10.1006/abio.2000.4706.

[15] M. Högbom, U.B. Ericsson, R. Lam, M.A. Bakali H., E. Kuznetsova, P. Nordlund, D.B. Zamble, A High Throughput Method for the Detection of Metalloproteins on a Microgram Scale, Mol. &Cellular Proteomics. 4 (2005) 827 LP-834. doi:10.1074/mcp.T400023-MCP200.

[16] D.R. Rosen, T. Siddique, D. Patterson, D.A. Figlewicz, P. Sapp, A. Hentati, D. Donaldson, J. Goto, J.P. O'Regan, H.X. Deng, et al., Mutations in Cu/Zn superoxide dismutase gene are associated with familial amyotrophic lateral sclerosis, Nature. 362 (1993) 59–62. doi:10.1038/362059a0.

[17] C. Soto, L.D. Estrada, Protein misfolding and neurodegeneration, Arch Neurol. 65 (2008) 184–

189. doi:10.1001/archneurol.2007.56.
[18] L.J. Hayward, J.A. Rodriguez, J.W. Kim, A. Tiwari, J.J. Goto, D.E. Cabelli, J.S. Valentine, R.H. Brown, Decreased metallation and activity in subsets of mutant superoxide dismutases associated with familial amyotrophic lateral sclerosis, J. Biol. Chem. 277 (2002) 15923–15931. doi:10.1074/jbc.M112087200.
[19] J.A. Rumfeldt, J.R. Lepock, E.M. Meiering, Unfolding and folding kinetics of amyotrophic lateral sclerosis-associated mutant Cu,Zn superoxide dismutases, J Mol Biol. 385 (2009) 278–298. doi:10.1016/j.jmb.2008.10.003.
[20] J.J. Goto, H. Zhu, R.J. Sanchez, A. Nersissian, E.B. Gralla, J.S. Valentine, D.E. Cabelli, Loss of in vitro metal ion binding specificity in mutant copper-zinc superoxide dismutases associated with familial amyotrophic lateral sclerosis, J Biol Chem. 275 (2000) 1007–1014. doi:10.1074/jbc.275.2.1007.
[21] H.L. Lelie, A. Liba, M.W. Bourassa, M. Chattopadhyay, P.K. Chan, E.B. Gralla, L.M. Miller, D.R. Borchelt, J.S. Valentine, J.P. Whitelegge, Copper and zinc metallation status of copper-zinc superoxide dismutase from amyotrophic lateral sclerosis transgenic mice, J. Biol. Chem. 286 (2011) 2795–2806. doi:10.1074/jbc.M110.186999.
[22] H.R. Broom, E.M. Meiering, H.A. Primmer, J.A.O. Rumfeldt, K.A. Vassall, P.B. Stathopulos, Y.-M. Hwang, Folding and aggregation of Cu, Zn-superoxide dismutase, INTECH Open Access Publisher, 2012. doi:10.5772/31629.
[23] C.M. Doyle, J.A. Rumfeldt, H.R. Broom, A. Broom, P.B. Stathopulos, K.A. Vassall, J.J. Almey, E.M. Meiering, Energetics of oligomeric protein folding and association, Arch Biochem Biophys. 531 (2013) 44–64. doi:10.1016/j.abb.2012.12.005.
[24] K.A. McCall, C. Huang, C.A. Fierke, Function and mechanism of zinc metalloenzymes, J Nutr. 130 (2000) 1437S–46S. doi:10.1093/jn/130.5.1437S.
[25] C.N. Pace, Determination and Analysis of Urea Guanidine Hydrochloride Denaturation Curves, Methods Enzymol. 131 (2016) 266–280. doi:10.1210/jc.20163294.
[26] E.D. Getzoff, D.E. Cabelli, C.L. Fisher, H.E. Parge, M.S. Viezzoli, L. Banci, R.A. Hallewell, R. Hallwell, R.A. Hallewell, Faster superoxide dismutase mutants designed by enhancing electrostatic guidance, Nature. 358 (1992) 347–351. doi:10.1038/358347a0.
[27] P.B. Stathopulos, J. a O. Rumfeldt, G.A. Scholz, R. a Irani, H.E. Frey, R. a Hallewell, J.R. Lepock, E.M. Meiering, Cu/Zn superoxide dismutase mutants associated with amyotrophic lateral sclerosis show enhanced formation of aggregates in vitro, Proc Natl Acad Sci U S A. 100 (2003) 7021–7026. doi:10.1073/pnas.1237797100.
[28] G. Labbé, J. Bezaire, S. de Groot, C. How, T. Rasmusson, J. Yaeck, E. Jervis, G.I. Dmitrienko, J. Guy Guillemette, High level production of the Magnaporthe grisea fructose 1,6-bisphosphate aldolase enzyme in Escherichia coli using a small volume bench-top fermentor, Protein Expr. Purif. 51 (2007) 110–119. doi:10.1016/j.pep.2006.06.020.
[29] T.J. Lyons, H. Liu, J.J. Goto, A. Nersissian, J.A. Roe, J.A. Graden, C. Cafe, L.M. Ellerby, D.E. Bredesen, E.B. Gralla, J.S. Valentine, Mutations in copper-zinc superoxide dismutase that cause amyotrophic lateral sclerosis alter the zinc binding site and the redox behavior of the protein, Proc Natl Acad Sci U S A. 93 (1996) 12240–12244. doi:10.1073/pnas.93.22.12240.
[30] D.R. Davydov, E. Deprez, G.H.B. Hoa, T. V. Knyushko, G.P. Kuznetsova, Y.M. Koen, A.I. Archakov, High-pressure-induced transitions in microsomal cytochrome P450 2B4 in solution: Evidence for conformational inhomogeneity in the oligomers, Arch. Biochem. Biophys. 320 (1995) 330–344. doi:10.1016/0003-9861(95)90017-9.
[31] P.B. Stathopulos, J.A.O. Rumfeldt, F. Karbassi, C.A. Siddall, J.R. Lepock, E.M. Meiering, Calorimetric analysis of thermodynamic stability and aggregation for Apo and Holo amyotrophic lateral sclerosis-associated Gly-93 mutants of superoxide dismutase, J. Biol. Chem. 281 (2006)

6184–6193. doi:10.1074/jbc.M509496200.
[32] J.A. Rumfeldt, P.B. Stathopulos, A. Chakrabarrty, J.R. Lepock, E.M. Meiering, Mechanism and thermodynamics of guanidinium chloride-induced denaturation of ALS-associated mutant Cu,Zn superoxide dismutases, J Mol Biol. 355 (2006) 106–123. doi:10.1016/j.jmb.2005.10.042.
[33] A. Kocyła, A. Pomorski, A. Krężel, Molar absorption coefficients and stability constants of metal complexes of 4-(2-pyridylazo)resorcinol (PAR): Revisiting common chelating probe for the study of metalloproteins, J. Inorg. Biochem. 152 (2015) 82–92. doi:10.1016/j.jinorgbio.2015.08.024.
[34] J.S. Valentine, P.A. Doucette, S. Zittin Potter, Copper-Zinc Superoxide Dismutase and Amyotrophic Lateral Sclerosis, Annu. Rev. Biochem. 74 (2005) 563–593. doi:10.1146/annurev.biochem.72.121801.161647.
[35] C. Tanford, Advances in Protein Chemistry, in: C.B. Anfinsen Jr, J. Edsall, F. Richards (Eds.), Academic Press, Inc, New York, 1970: pp. 2–97.
[36] S.M. Lynch, S.A. Boswell, W. Colón, Kinetic stability of Cu/Zn superoxide dismutase is dependent on its metal ligands: Implications for ALS, Biochemistry. 43 (2004) 16525–16531. doi:10.1021/bi048831v.
[37] J.R. Jezorek, H. Freiser, 4-(Pyridylazo)resorcinol)-based continuous detection system for trace levels of metal ions, Anal. Chem. 51 (1979) 373–376. doi:10.1021/ac50039a012.
[38] H. Liu, H. Zhu, D.K. Eggers, A.M. Nersissian, K.F. Faull, J.J. Goto, J. Ai, J. Sanders-Loehr, E.B. Gralla, J.S. Valentine, Copper(2+) binding to the surface residue cysteine 111 of His46Arg human copper-zinc superoxide dismutase, a familial amyotrophic lateral sclerosis mutant, Biochemistry. 39 (2000) 8125–8132. doi:10.1021/bi000846f.
[39] J.A. Rodriguez, J.S. Valentine, D.K. Eggers, J.A. Roe, A. Tiwari, R.H. Brown Jr., L.J. Hayward, Familial amyotrophic lateral sclerosis-associated mutations decrease the thermal stability of distinctly metallated species of human copper/zinc superoxide dismutase, J Biol Chem. 277 (2002) 15932–15937. doi:10.1074/jbc.M112088200.
[40] Q. Wang, J.L. Johnson, N.Y.R. Agar, J.N. Agar, Protein aggregation and protein instability govern familial amyotrophic lateral sclerosis patient survival, PLoS Biol. 6 (2008) e170. doi:10.1371/journal.pbio.0060170.
[41] H.R. Broom, J.A.O. Rumfeldt, E.M. Meiering, Many roads lead to Rome? Multiple modes of Cu,Zn superoxide dismutase destabilization, misfolding and aggregation in amyotrophic lateral sclerosis., Essays Biochem. 56 (2014) 149–65. doi:10.1042/bse0560149.
[42] J.A. Fee, Studies on the reconstitution of bovine erythrocyte superoxide dismutase. IV. Preparation and some properties of the enzyme in which Co(II) is substituted for Zn(II), J Biol Chem. 248 (1973) 4229–4234.

Appendix

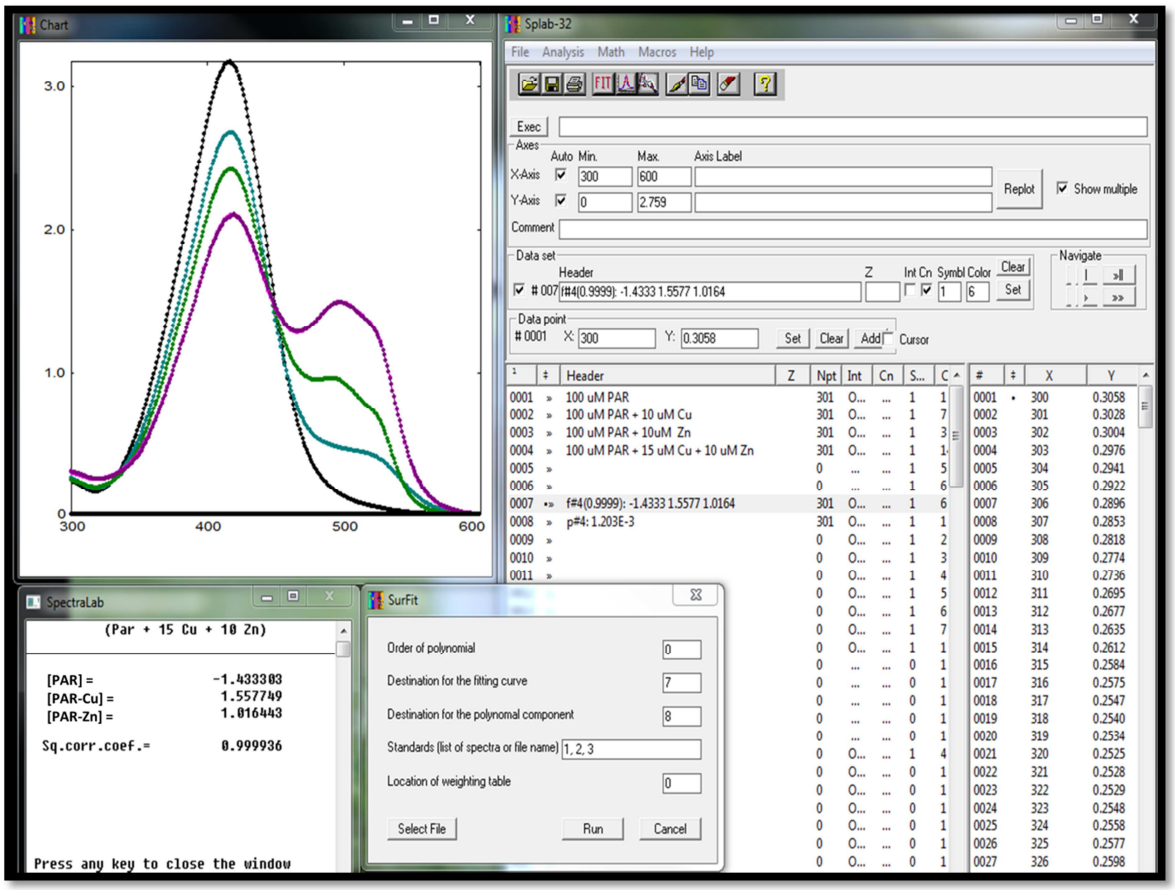

Figure A.1 - Screenshot of SpLab software [30]. Experimental data should be saved as a comma delimited (*.csv) file in Excel. Multiple spectra can be saved in one file by having the experimental data arranged by column. For analysis, absorbance data from 300 nm to 600 nm is used. When SpLab is open (large right panel), under the "File" tab select "Load ASC, CSV or DAT File…" to load the experimental data into the program. Select the row which represents the spectrum you would like to fit and under the Data Analysis tab there is an option for "Spectral Decomposition". This will open the SurFit window (bottom middle panel) where one can select the standard spectra (by row) for fitting the experimental spectrum and the destination for the fitted curve. The order of the polynomial should be set to 0. Upon clicking 'run' a SpectraLab window will appear (bottom left panel) which gives the fraction (weighting coefficients) of each standard spectrum in the fitted spectrum. The quality of the fit is also given in this window by the squared correlation coefficient. The standard spectra of 100 µM PAR, PAR:Cu (10 µM) and PAR_2:Zn (10 µM) are shown in the upper left panel in black, teal and green, respectively. The experimental spectrum is shown in purple (15 µM Cu^{2+}, 10 µM Zn^{2+}). The fitted spectrum is also plotted but is not visible as it lies directly under (i.e. is effectively coincident with) the experimental spectrum.

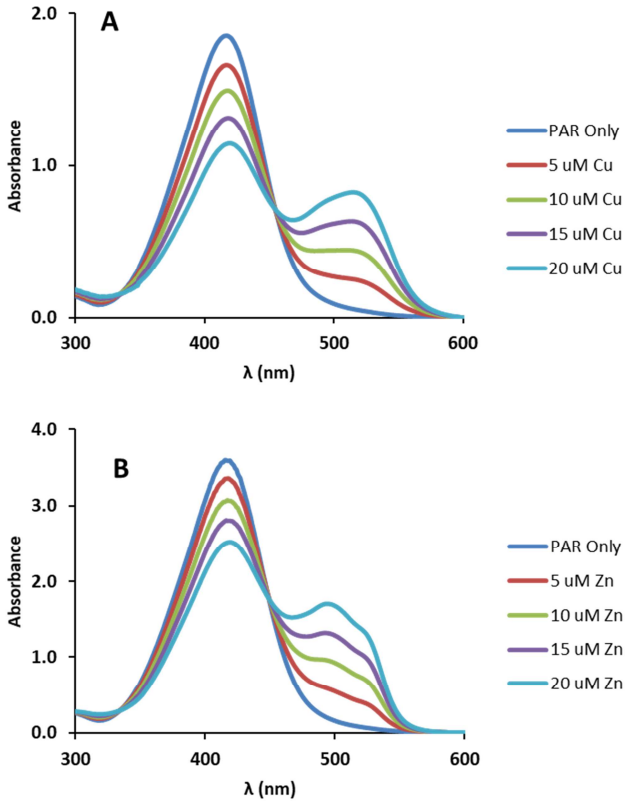

Figure A.2 Quantification of a Single Metal Species with PAR. Experimental spectra for samples of increasing known concentrations of Cu^{2+} **(A)** or Zn^{2+} **(B)** in 50 µM PAR .

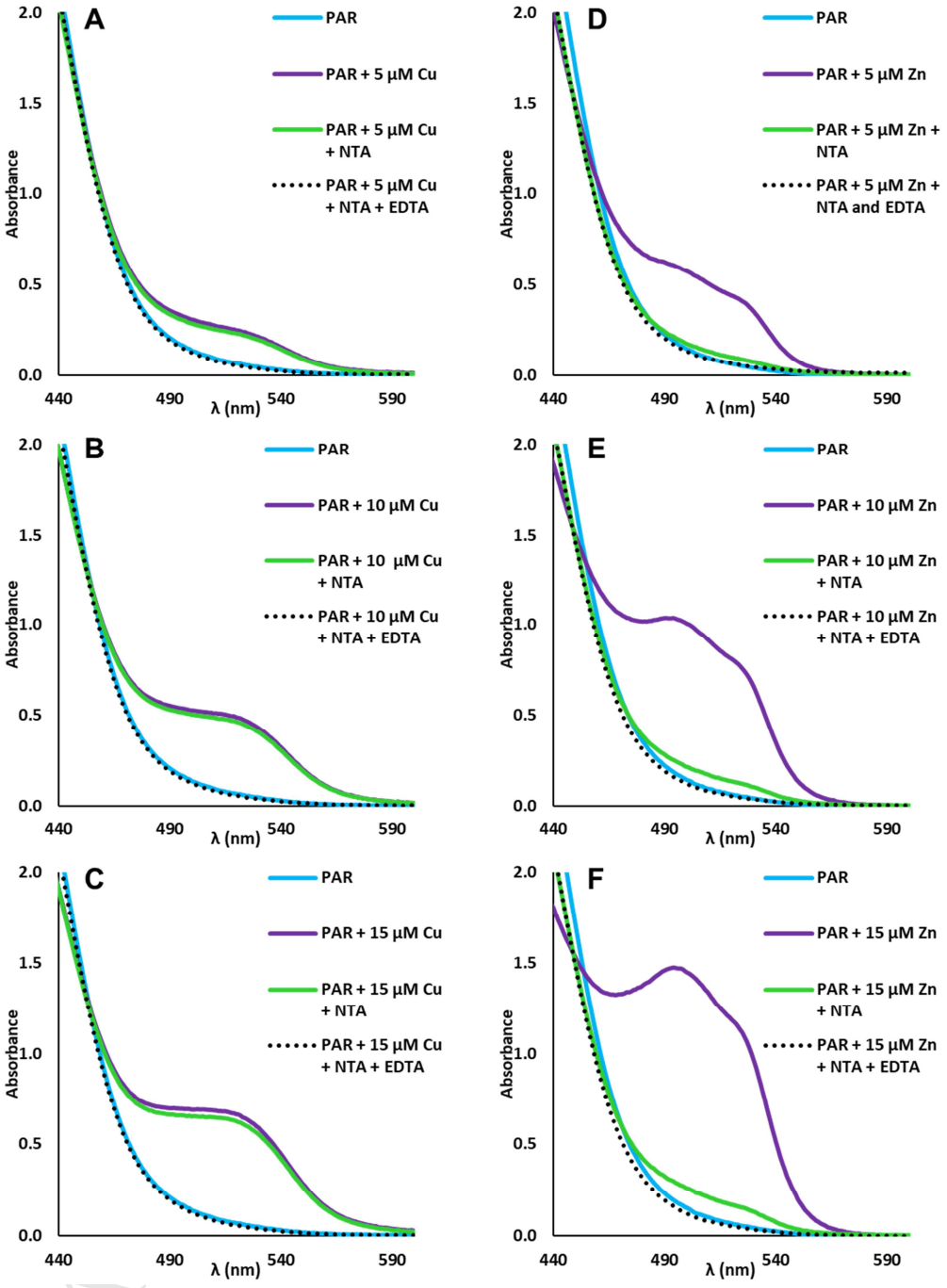

Figure A.3. Specificity of the chelators used in previous PAR assay for simultaneous Cu^{2+} and Zn^{2+} determination. In this assay, the decrease in absorbance at 500nm (ΔAbs_{500}) is converted to the concentration of metal bound by each chelator using the Beer-Lambert law and the corresponding extinction coefficient [9]. (A),(B), and (C) Changes in the absorption spectrum of PAR (100 µM) with Cu^{2+} (5 µM, 10 µM and 15 µM, respectively), upon addition of NTA (0.8 mM) (green) followed by EDTA (0.8 mM) (dotted line). (D), (E), and (F) Changes in the absorption spectrum of PAR (100 µM) with Zn^{2+} (5 µM, 10 µM and 15 µM, respectively), upon addition of NTA (0.8 mM) and then EDTA (0.8 mM).

Table A.1. Quantification of a Single Metal Species: Determination of Cu^{2+} and Zn^{2+} in solution using PAR assay protocol

Known concentration (µM)		Calculated concentration (µM)		Calculated % metal	
Cu^{2+}	Zn^{2+}	Cu^{2+}	Zn^{2+}	Cu^{2+}	Zn^{2+}
5.0	0.0	4.98	0.068	99.5%	
10.0	0.0	10.00	0.000	100.0%	
15.0	0.0	15.03	0.006	100.2%	
20.0	0.0	20.05	0.029	100.3%	
25.0	0.0	24.94	-0.097	99.8%	
0.0	5.0	-0.016	5.08		101.6%
0.0	10.0	0.000	10.00		100.0%
0.0	15.0	0.119	14.75		98.3%
0.0	20.0	0.238	19.81		99.1%
0.0	25.0	0.577	24.40		97.6%

Experiment was conducted as described, but without the addition of a second metal. Spectral deconvolution routine for all samples was conducted using PAR, PAR:Cu^{2+}, and PAR2:Zn^{2+} spectra. The percent (%) metal was calculated as ([calculated metal] / [known metal])*100%.

Table A.2. Accuracy and precision of the simultaneous determination of Cu^{2+} and Zn^{2+} in solution using PAR assay protocol with NTA and EDTA (8)

Known concentration (µM)		Calculated concentration (µM)		Calculated % metal	
Cu^{2+}	Zn^{2+}	Cu^{2+}	Zn^{2+}	Cu^{2+}	Zn^{2+}
5.0	20.0	10.8 ± 1.2	15.7 ± 0.8	215 ± 24	78 ± 4
10.0	15.0	12.8 ± 0.8	13.1 ± 0.2	128 ± 8	88 ± 2
15.0	10.0	16.6 ± 0.6	8.8 ± 0.1	110 ± 4	88 ± 1
20.0	5.0	19.4 ± 0.5	5.0 ± 0.1	97 ± 2	100 ± 2
5.0	5.0	6.4 ± 0.8	4.6 ± 0.2	128 ± 16	92 ± 3
10.0	10.0	11.5 ± 0.4	9.1 ± 0.2	115 ± 4	91 ± 2

Each value represents the mean ± the deviation of two independent sample measurements. The percent (%) metal was calculated as ([calculated metal] / [known metal])*100%. All samples contained 100 µM PAR, 5.4 M GdnHCl, 50 mM HEPES, pH 8.2. These experiments were completed in 20 mM Hepes at pH 8.2, which is comparable to the solution conditions outlined by Crow *et al.* [9] (0.1 M sodium borate, pH 7.8).

HIGHLIGHTS

- A multicomponent PAR assay is developed to measure multiple metal ions concurrently
- Zn^{2+} and Cu^{2+} concentrations in SOD1 samples were determined accurately and precisely
- ALS-associated SOD1 mutants are found more likely to be under- or mis-metallated
- Contaminating EDTA limits metal quantitation using 4-(2-pyridylazo)resorcinol (PAR)